DIELECTRIC SPECTROSCOPY AND CALORIMETRY IN THE GLASS TRANSITION REGION OF SEMI-CRYSTALLINE POLY(ETHYLENE TEREPHTHALATE)

*J. Dobbertin, A. Hensel and C. Schick**

Department of Physics, University of Rostock, Universitätsplatz 3, D-18051 Rostock, Germany

Abstract

Confinement of the glass-forming regions in the nanometer range influences the α-relaxation which is associated with the glass transition. These effects were investigated for semicrystalline poly(ethylene terephthalate) by dielectric spectroscopy and differential scanning calorimetry. The results are discussed within the concept of cooperative length, i.e. the characteristic length of the cooperative process of glass transition. Both experiments showed a dependence of the glass transition on the mean thickness of the amorphous layers. For the dielectric relaxation, the loss maximum was found to shift to higher temperatures with decreasing thickness of the amorphous layers, but no differences were observed in the curve shape for the differently crystallized samples. For the calorimetric measurements, in contrast, there was no correlation for the glass transition temperature, whereas the curve shape did correlate with the layer thickness of the mobile amorphous fraction. From the structure parameters, a characteristic length of approximately (2.5 ± 1) nm was estimated for the unconfined glass relaxation (transition).

Keywords: dielectric relaxation, differential scanning calorimetry (DSC), glass transition, main relaxation, semicrystalline polymers, poly(ethylene terephthalate)

Introduction

The glass transition is at present a central problem of condensed matter physics, but there is no generally accepted theory for it. The investigation of glass-forming liquids in geometries of confining length could give a deeper insight into the nature of the glass transition [1]. In this paper, we discuss thermal and dynamic glass transitions in confined amorphous regions of semicrystalline polymers.

To describe the glass transition, the idea of molecules rearranging themselves cooperatively within regions of characteristic size [2] has been found to be very attractive. This concept is at the center of discussions concerning the

---

* Author to whom all correspondence should be addressed.

glass transition and there is growing interest in relating it to measurable physical quantities [3]. Donth *et al.* [4–6] estimated the length of cooperativity to be a few nm ($\xi \approx 2$–3 nm). However, direct experimental verification of equilibrium is not possible at present, because there are no time-resolving scattering methods for frequencies $v < MHz$ on the nanometer scale. Therefore, we must try to use indirect experimental methods to estimate the characteristic length range. By confining a glass-forming liquid into small volumes of the dimensions of a few nm^3, it should be possible to get information on its cooperativity length. This means that on decrease of the dimensions of the glass-forming regions below the dimensions of the cooperatively rearranging regions (diameter $< 2\xi$), a different relaxation behaviour in comparison to that of the bulky amorphous material should appear.

Investigations of the glass transition in confined liquids have been published recently [3, 7–9]. In all these papers, controlled porous glasses were used to investigate the influence of size effects on relaxation dynamics. The results were conflicting. Both a decrease [3, 7] and a small increase [8] in the dynamic glass transition temperature due to restriction was found. An increase in the glass transition temperature is in accordance with the theoretical prediction of Sappelt and Jäckle [1]. They pointed out that the confinement of glass-forming liquids in geometries of confining length comparable to the cooperativity length ξ should lead to a broadening of the glass transition and a shift to higher temperatures.

To test this hypothesis, we have used the confinement of the glass-forming regions by the semicrystalline morphology of a polymer. In semicrystalline polymers, the amorphous regions will be restricted by the crystalline lamellae and the corresponding interfacial regions. As compared to controlled porous glasses [9], only small effects related to surface interactions should appear, because the restriction of the glass-forming regions is due to the same substance. In the present paper, we compare the glass transition in the amorphous regions within the semicrystalline morphology with the bulky glass transition of the same polymer in the fully amorphous state. By varying the size of the amorphous regions, d_{am}, one can investigate whether and how both the thermal (vitrification) and the dynamic glass transition are influenced. Therefore, it is first necessary to determine the dimensions of the regions which participate in the glass transition. As introduced by Ishida [10] for dielectric and Wunderlich [11] for calorimetric investigations, the fraction participating in the glass transition can be determined by the intensity of the relaxation process under investigation ($\Delta\varepsilon$, Δc_p; etc.) [4, 12]. We will compare the results of calorimetric investigations on the vitrification process (Δc_p) with those of dielectric spectroscopy for the main relaxation process ($\Delta\varepsilon$). The thickness of the layers participating in the glass transition is then calculated by using a one-dimensional layer stack model, as is often done for the interpretation of small-angle X-ray scattering (SAXS) data [13].

As reported earlier [4, 14], there is a correlation between the correlation length ξ extracted from the shape of the c_p curve in the glass transition region according to Donth [15] and the thickness of the amorphous layers for semicrystalline poly(ethylene terephthalate) (PET). The investigation results in a cooperativity length for the unconfined thermal glass transition of the order of 2 nm [4]. This paper aims to compare the results of calorimetry with those of dielectric spectroscopy.

Sample characterization

Determination of amorphous layer thickness

As described previously [4], semicrystalline PET forms amorphous regions with dimensions of the order of the cooperativity length ξ. Semicrystalline flexible polymers exhibit a typical structure, with crystalline lamellae (index c), interfacial or rigid amorphous (index ar) and mobile amorphous (index am) layers (Fig. 1). To determine the morphological parameters by using a one-dimensional layer stack model, three assumptions must first be fulfilled:

(i) The sample is completely filled with the stack structure of Fig. 1. If the semicrystalline sample is fully crystallized (this means as much as possible), then non-crystalline regions are present only between the lamellae.

(ii) The lateral layer extension is much larger than its thickness (d_{am}, d_{ar}, d_c). The layer thickness can then be determined from the one-dimensional layer stack model *via* Eq. (3).
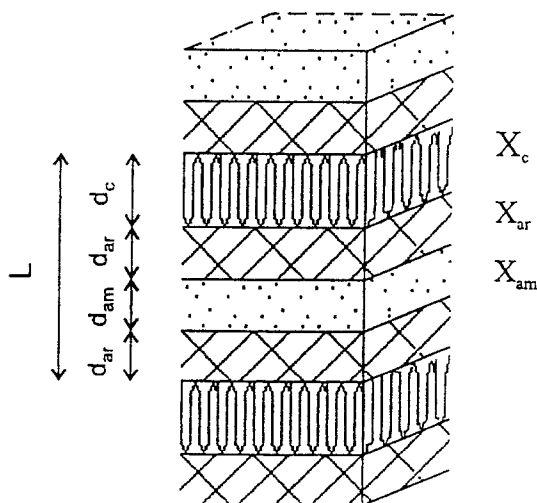

Fig. 1 Stack of lamellae in semicrystalline polymers. χ... Volume fraction; d...layer thickness; Index c...crystalline, ar...amorphous rigid, am...amorphous mobile

(iii) The layers are homogeneous. Non-crystalline parts inside the lamellae are associated with the rigid amorphous material.

In such a completely crystallized semicrystalline sample as described above, only intraspherulitic amorphous regions exist between the lamellae, and no interspherulitic amorphous regions [16, 17]. This means that we can observe the glass transition within the mobile amorphous regions (d_{am}) between the lamellae [12], the thickness of which can be determined via Eq. (3).

Investigation of the relaxation intensity in most semicrystalline polymers with crystalline mass fraction χ_c shows that not all of the non-crystalline fraction $(1-\chi_c)$ participates in the glass transition [18]. Therefore, a rigid amorphous (χ_{ar}) and a mobile amorphous (χ_{am}) fraction have been postulated [11]. The mobile amorphous fraction χ_{am}, which contributes to the glass transition, can be determined by using different methods, from the ratio between the relaxation intensity of the sample under test and the relaxation intensity of a 100% amorphous sample. Wunderlich's group developed this method [11], considering the intensity of the thermal glass transition

$$\chi_{am} = \frac{\Delta c_p}{\Delta c_{pa}} \qquad (1)$$

where Δc_p is the step height of the specific heat capacity at the glass transition for the sample under test, and Δc_{pa} is that for a totally amorphous sample. The rigid amorphous fraction can be calculated from

$$\chi_{ar} = 1 - \chi_c - \chi_{am} \qquad (2)$$

The long period L of the samples was determined from the one-dimensional electron density correlation function as measured by SAXS [19, 20]. According to the one-dimensional layer stack model, the layer thickness can be evaluated by the product L times volume fraction:

$$d_c = LX_c \qquad 2d_{ar} = LX_{ar} \qquad d_{am} = LX_{am} \qquad (3)$$

The volume fractions (X) can be determined from the mass fractions (χ) through multiplication by the density ratio ρ/ρ_a (or ρ/ρ_c for the crystalline region), where ρ is the density of the sample under test, ρ_a is the density of the amorphous fraction, and ρ_c is the crystalline density. The mass crystallinity fraction χ_c can be determined by wide-angle X-ray scattering (WAXS), melting enthalpy, density or NMR methods. In the following, we have used the fraction χ_c from WAXS.

Variation of amorphous layer thickness

Using different temperature–time programs, one can generate semicrystalline structures with different morphologies [20–23].

From one PET batch (ORWO K 36, $\overline{M}_w \approx 23000$), we prepared two series of samples with a variation of the thickness of the mobile amorphous layers of between approximately 1.8 nm and 3.3 nm.

The first sample series which we prepared used isothermal crystallization in the temperature range $T_c = 120$ to 220°C (3...18 h depending on the growth rate). Both long period L and crystallinity χ_c increase with increasing T_c [22], whereas the fraction χ_{am} remains nearly constant [24].

The second series was prepared by gradual crystallization according to Groeninckx [23]. First, the sample was completely crystallized (18 h) at $T_c = 120$°C. Then, the sample was heated at a rate of $q = 0.1$ K min^{-1} up to the next annealing temperature, T_a, e.g. $T_a = 140$°C, at which the sample was additionally annealed for a period of 18 h. After that, the sample was heated again at the same rate q up to the next annealing temperature T_a, and again annealed for 18 h. This procedure was repeated until the final annealing temperature T_a was reached. In the gradually crystallized series, no variation of the long period, fixed by the first annealing at 120°C, was observed for T_a less than 220°C [20, 23]. The crystallinity χ_c increases with increasing annealing temperature, similarly as in the first series.

The structure parameters determined for the two series are shown in Table 1.

Table 1 Layer fractions and thicknesses for the prepared PET samples

Sample	Crystallization regime	χ_c	χ_{ar}	χ_{am}	$d_c/$	$2d_{ar}/$	$d_{am}/$
						nm	
iso 120	18 h 120°C	0.25	0.4	0.35	1.8	3.2	2.8
iso 140	6 h 140°C	0.26	0.38	0.36	2	3.2	3
iso 160	3 h 160°C	0.27	0.37	0.36	2.3	3.3	3.2
iso 180	3 h 180°C	0.30	0.34	0.36	2.6	3.1	3.3
iso 200	5 h 200°C	0.34	0.32	0.34	3.1	3.1	3.3
iso 220	10 h 220°C	0.36	0.33	0.31	3.6	3.4	3.2
gra 140	gradual to 140°C	0.26	0.41	0.33	1.9	3.3	2.7
gra 160	gradual to 160°C	0.27	0.42	0.31	2	3.4	2.5
gra 180	gradual to 180°C	0.29	0.43	0.28	2.2	3.4	2.2
gra 200	gradual to 200°C	0.33	0.42	0.25	2.5	3.4	2
gra 220	gradual to 220°C	0.37	0.41	022	2.8	3.3	1.8

Experimental

Dielectric measurements

The dielectric measurements were carried out in the frequency range 0.01 Hz to 1 MHz with a BDS 4000 broad band dielectric spectrometer (Novocontrol GmbH). A frequency response analyzer SI 1260 (Solatron-Schlumberger), which was supplemented by using a high-impedance preamplifier of variable gain, was used to extract the complex dielectric function $\varepsilon^*(\omega)$. The sample was kept between two condenser plates in a cryostat. The sample temperature was controlled by using a heated N_2 gas stream. Frequency scans were performed at constant temperature, with a stability better than 0.1 K. The temperature scale was checked via the melting point of indium. The deviation from the expected melting point was less than 0.5 K.
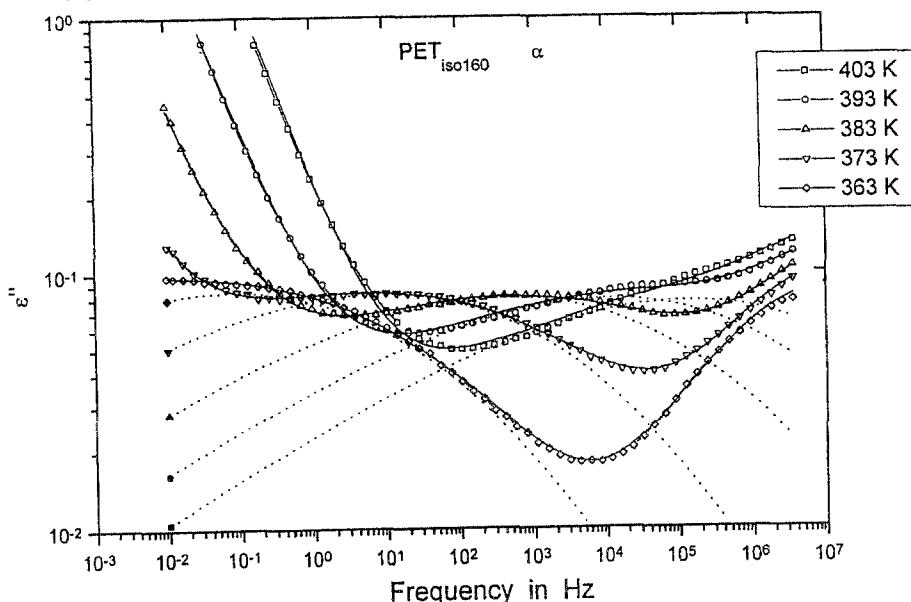

Fig. 2a Real part of the complex dielectric function in the glass transition region of PET for the sample isothermally crystallized for 3 h at 160°C. The solid lines through the data represent the fit using two superimposed HN functions (α- and β-relaxation) and $A_1 \cdot \omega^{-n_1}$ for Maxwell-Wagner-Sillars polarization. The dashed lines show the HN fit for α-relaxation

Figure 2 shows typical frequency scans for semicrystalline PET samples. The measured dielectric function can be described quantitatively by generalized relaxation functions. The most general one is the Havriliak-Negami (HN) equation [25]:

$$\varepsilon^*(\omega) = \varepsilon_\infty + \frac{\varepsilon_{st} - \varepsilon_\infty}{(1 + (i\omega\tau)^\beta)^\gamma} \qquad (0 < \beta, \beta\gamma \leq 1) \qquad (4)$$

β and γ are shape parameters; ω is the angular frequency of the applied field $\omega = 2\pi\nu$; τ is the characteristic relaxation time; and $\Delta\varepsilon = \varepsilon_{st} - \varepsilon_\infty$ is the relaxation strength ($\varepsilon_{st} = \varepsilon'(\omega)$ for $\omega \ll 1/\tau$; $\varepsilon_\infty = \varepsilon'(\omega)$ for $\omega \gg 1/\tau$). The relaxation time τ depends to some extent on the shape parameters β and γ. The frequency of the dielectric loss maximum ν_{max}, with $\nu_{max} = (2 \pi\tau_{max})^{-1}$, is independent of the shape parameters and has been used in the following as the relaxation frequency. The α-relaxation is influenced by neighboring processes, conductivity on the low-frequency tail and secondary relaxation on the high-frequency tail. These processes must be included in the fitting procedure [26]. Figures 2a and 2b show the real and imaginary parts of the complex dielectric function for a sample crystallized isothermally at $T_c = 160°C$.
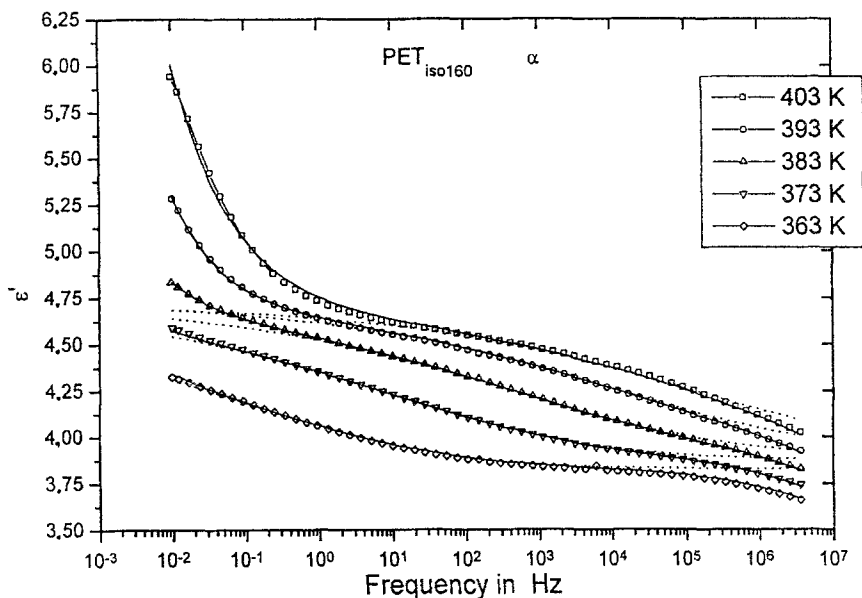

Fig. 2b Imaginary part of the complex dielectric function in the glass transition region of PET for the sample isothermally crystallized for 3 h at 160°C. The solid lines through the data represent the fit using two superimposed HN functions (α- and β-relaxation) and $A_2 \cdot \omega^{-n_2}$ for the conductivity contribution. The dashed lines show the HN fit for the α-relaxation. The parameters for α- and β-relaxation used in Figs 2a and 2b are the same

Calorimetric measurements

The parameters of the thermal glass transition were determined by using a Perkin-Elmer DSC-7 differential scanning calorimeter. The temperature scale

of the calorimeter was calibrated with indium and lead for the scanning rate under investigation and for the heat flow by sapphire. The purge gas was nitrogen. The temperature of the calorimeter block and also the room temperature were kept well stabilized in order to achieve reproducible scans.

In these measurements, the sample mass was about 15 mg and the scanning rate was 10 K min^{-1} for both heating and cooling. The sample was first cooled from the corresponding crystallization temperature to 280 K in order to erase the thermal history relating to the glass transition. From the heating scan, which immediately followed, the glass transition temperature T_g was determined to be the temperature of the half step in c_p, the intensity of the glass transition, Δc_p, being the difference between the tangents at T_g (see inset in Fig. 3). The heat capacities for various representative samples are plotted in Fig. 3.
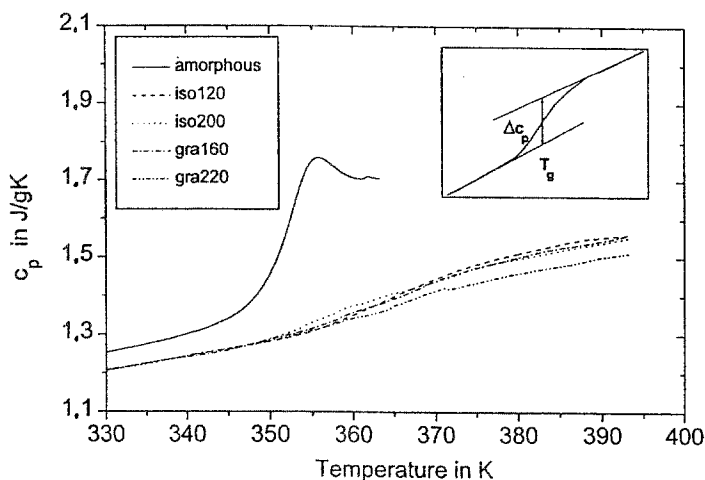

Fig. 3 DSC curves in the glass transition region for differently crystallized PET samples (Table 1)

Results and discussion

Analogously to Eq. (1), the dielectric intensity can be normalized to the intensity of the mobile amorphous fraction by

$$\chi_{am}^{dielec} = \frac{\Delta\varepsilon}{\Delta\varepsilon_a} \tag{5}$$

Comparison of thermal and dynamic glass transition intensities reveals similar behavior (Fig. 4). In both experiments, we found that the relaxation intensity ($\Delta\varepsilon$, Δc_p) of the non-crystalline fraction ($1 - \chi_c$) of the sample is smaller than expected. Such a quantitative analysis shows that there is a non-crystalline fraction

which does not contribute to the relaxation intensity. There are other results [27] which suggest that the differences observed from the two-phase model result from a wrong determination of the crystallinity. To test this, we also determined the dielectric strength of the secondary relaxation process (β-relaxation).
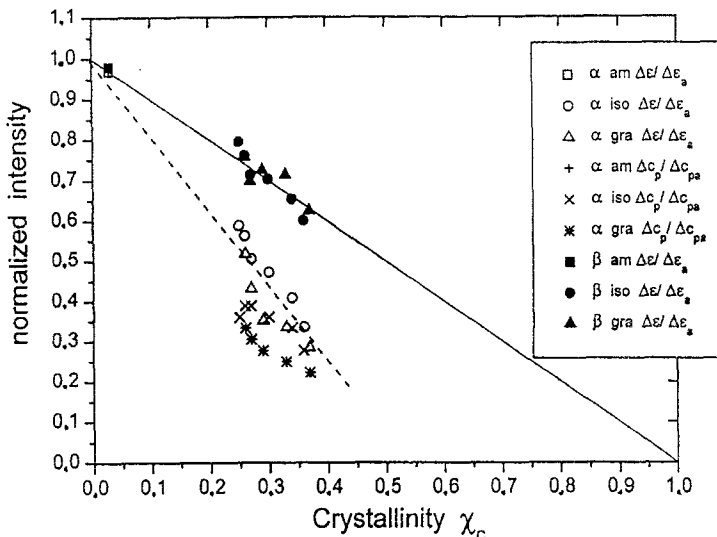

Fig. 4 Normalized intensity for α- (ε, c_p) and β-relaxation (ε) for differently crystallized PET samples (Table 1)

The β-relaxation is connected with the local movements of the main chains. Such local movements could be expected to occur in the whole non-crystalline part because these movements are only slightly influenced through the confining crystalline lamellae. This is why the secondary relaxation should follow the two-phase model ($\Delta\varepsilon\approx1-\chi_c$). Figure 4 compares the normalized dielectric intensities for the α- and the β-relaxation. We found the expected dependence for the β-relaxation. This shows that the deviations from the two-phase model for the α-relaxation are the result of a rigid amorphous fraction. This means that a local movement is possible in the rigid amorphous fraction, but not a cooperative segmental motion (α-relaxation, glass transition) [10].

A direct comparison of the mobile amorphous fractions found by DSC and dielectric measurements is difficult. The dielectric intensity was determined for each sample at the temperature which results in a frequency of 100 Hz for the loss maximum (same relaxation time). For the DSC experiment, such an exact assignment is not possible. From a relationship between cooling rate and relaxation frequency [15, 28], a frequency of nearly 10^{-3} Hz can be estimated for the thermal glass transition at a cooling rate of 10 K min^{-1}.

In the dielectric experiment, the relaxation strength for the α-relaxation decreases with increasing temperature. This decrease can be observed especially

for the amorphous sample. For the semicrystalline sample, a nearly temperature-independent relaxation strength was found. Consequently, the normalized relaxation strength $(\Delta\varepsilon/\Delta\varepsilon_{am})$ depends on the temperature of the dynamic glass transition, which depends on frequency. With increasing frequency or temperature, the normalized relaxation strength increases. To compare the normalized relaxation strengths of dielectric and caloric relaxation, both measurements must be performed at the same frequency. With the help of temperature-modulated calorimetry, it would be possible to perform such measurements in the future. Another reason to use the normalized relaxation strength from calorimetric measurements for the determination of the mobile amorphous fraction is the fact that calorimetry covers the response of all modes (degrees of freedom). In contrast, the dielectric response is related to the movement of an electric dipole and not all modes are connected with such a movement.

In the present paper, therefore, the mobile amorphous fraction is determined by the normalized step height of the specific heat capacity at the thermal glass transition for a heating rate of 10 K min^{-1}. The thickness of the mobile amorphous layers within which the glass transition takes place is determined through Eq. (3). For the samples under investigation, a layer thickness of from 1.8 nm to 3.3 nm was estimated. The uncertainty of the absolute values is relatively high, possibly up to 50%, due to the very simple model and also to the uncertainty in the determination of both the long period L and the step height of the specific heat capacity Δc_p. Nevertheless, the tendency of the layer thickness variation in the nanometer range is only slightly influenced by this uncertainty.
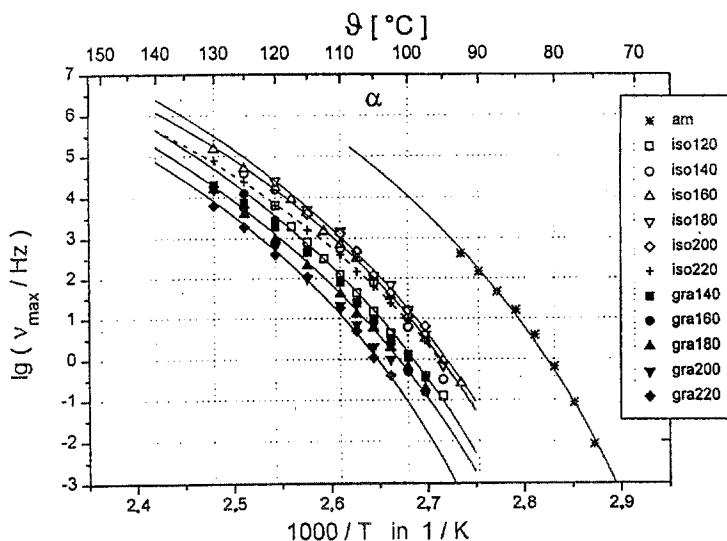

Fig. 5 Arrhenius diagram for the dielectric α-relaxation of amorphous (stars) and semicrystalline PET samples (Table 1). Lines correspond to a VFT equation

With use of the concept of cooperativity length, a confinement of the glass-forming regions in the nanometer range should influence the relaxation behavior. According to Sappelt and Jäckle [1], the confinement of glass-forming liquids in geometries of confining length comparable to the cooperativity length should lead to a broadening of the glass transition and a shift to higher temperatures. For differently crystallized PET, we found an isochronal (constant-frequency) shift of the loss maximum (dynamic glass temperature) in the Arrhenius diagram (Fig. 5). This shift correlates with the thickness of the mobile amorphous layers (Fig. 6). A decrease in the thickness of the mobile amorphous layers results in an increase in the dynamic glass temperature. The thermal glass temperature, determined by DSC, does not seem to follow this dependence. However, there is a difference in the determination of the thermal and the dynamic glass temperature. For the thermal experiment, we can not assume that we measure at the same frequency. It is well known that there is a relationship between the cooling rate and the observed glass transition temperature. Also, there is a relationship between the cooling rate and the relaxation frequency [15]. We earlier showed [28] that it is necessary to include the mean temperature fluctuation in this relationship. For semicrystalline PET, it was found that the mean temperature fluctuation depends strongly on the thickness of the mobile amorphous layers [14]. This means that the differences in Fig. 6 can be a result of the different measurement conditions.
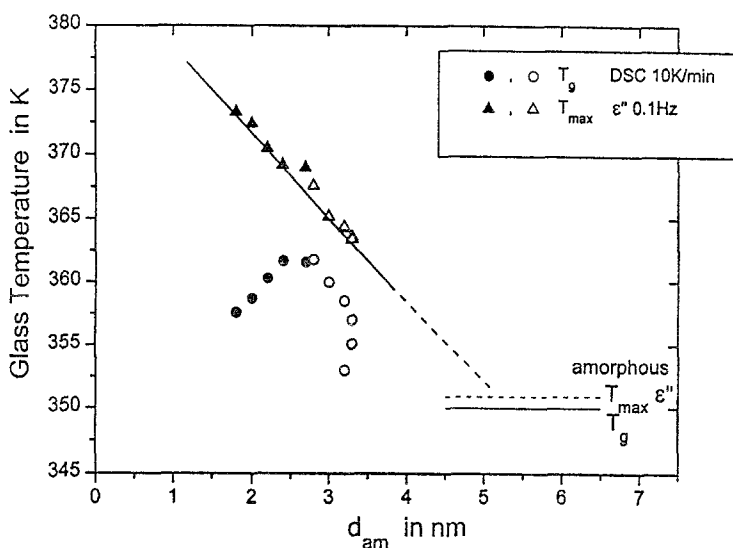

Fig. 6 Dynamic (temperature of dielectric loss maximum at $f_{max} = 0.1$ Hz) and thermal glass temperatures as a function of the thickness of the mobile amorphous layers. Full symbols represent gradually crystallized samples; open symbols represent isothermally crystallized samples (Table 1)

An analysis of the shape of the α-loss peaks revealed no differences between the differently crystallized samples. However, we found a significantly broader α-loss peak in the semicrystalline than in the amorphous samples (Fig. 7). According to the concept of cooperativity length, only the low-frequency tail is influenced by the restriction of the glass-forming regions. The high-frequency tail is not influenced. This result therefore lends strong support to the concept of a cooperative glass transition [15, 29] in which the cooperative motion may be described by a great variety of modes of different spatial extents. In this concept, the high-frequency tail is mainly determined by short-range modes and the low-frequency tail by long-range modes [30]. As shown in Fig. 7, the high-frequency tails are not influenced by the geometrical restriction due to the crystals because of the short mode length. For these molecular motions, it is of little interest whether or not the crystals are located at a relatively long distance as compared to the mode length. The motions detected at low frequencies are associated with long mode length (long distance fluctuations), which are comparable to the dimensions of the mobile amorphous regions in the semicrystalline samples. Because of the geometrical confinement caused by the crystals, the mode length is restricted to the geometrical length. To attain all molecular movements necessary for the glass transition, the molecules have to find other ways than those related with the long mode length. This means that the conformational changes which occur in the semicrystalline sample will be carried out by the molecules in a way that needs more time. In turn, the result is that the low-frequency tail (corresponding to long times) is broadened.
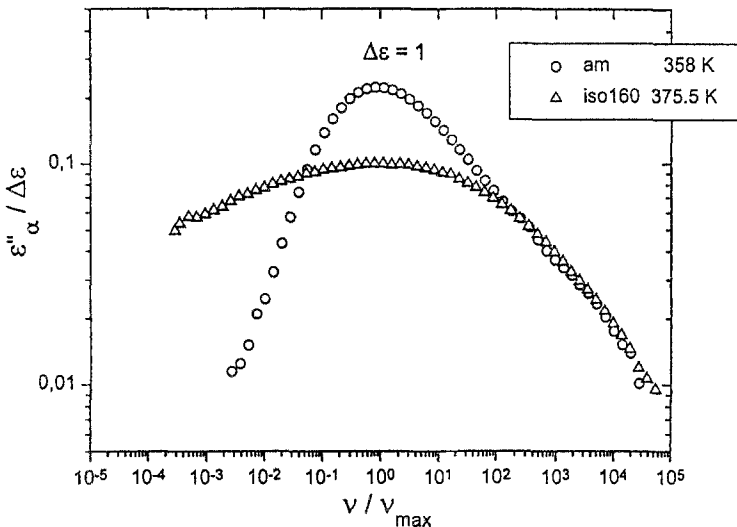

Fig. 7 α-loss peak (conductivity and secondary relaxation are subtracted) normalized to the same intensity ($\Delta\varepsilon = 1$) for amorphous and semicrystalline (iso 160) PET. The frequency axis is normalized to the peak position ($f_{max} \approx 25$ Hz)

Preliminary measurements with a temperature-modulated calorimeter [28] can be discussed in the same way. An isochronal temperature scan of the complex heat capacity shows a much broader high-temperature tail, which corresponds to low frequencies for the semicrystalline sample than for the amorphous one. The low-temperature tail is influenced non-significantly.

Conclusions

The geometrical confinement of the glass-forming regions in semicrystalline polymers is one way to determine the cooperativity length of the glass transition. The simple idea is to determine the dimensions of the glass-forming regions at which the disturbance of the glass transition due to the confinement starts. At the moment, it is not possible to observe directly the change from an undisturbed glass transition to a disturbed one. The reason for this is that we do not know any substance where we can vary the dimensions of the glass-forming regions between approximately 6 nm and 3 nm. From our dielectric and calorimetric investigations on semicrystalline PET, we observe a correlation between the parameters of the glass transition and the thickness of the mobile amorphous layers. This layer thickness varies between approximately 1.8 nm and 3.3 nm. Extrapolation of the layer thickness dependence of the maximum position of the dielectric loss to the value for the bulky amorphous sample results in a layer thickness of about 5 nm. For layer thicknesses smaller than 5 nm, the confinement of the glass-forming regions should influence the cooperative movements. From this, we can estimate the correlation length of the undisturbed dielectric glass relaxation to be about 2.5 nm. From the calorimetric investigations on the same samples, we observe a dependence of the width of the glass transition range (curve shape) upon the layer thickness [4, 14], but no correlation of the glass transition temperature (Fig. 6). Extrapolation of the curve shape parameters to the bulky amorphous value yields slightly more than 3 nm [4]. Our results of 2.5 nm from dielectric relaxation and 1.6 nm from calorimetry are within the error limits of both extrapolations. Therefore, it is not possible to discuss any differences between the two measurements. However, we can conclude that both independent measurements yield a correlation length of some nm for the undisturbed glass relaxation (transition). This is in agreement with the predictions of different theories [15, 31] and is independent of any calculation relating to the theories.

The reason for the differences between the dielectric and calorimetric observations is not known at the moment. We found for the dielectric measurements a dependence of the location of the maximum of the loss peak (dynamic glass transition temperature), but no influence of the layer thickness on the curve shape for the semicrystalline samples. In contrast, in the calorimetric investigation we observed no correlation between the glass transition temperature and the layer thickness, but a dependence of the curve shape upon the layer thickness. One reason for this different behavior may be the different measuring con-

ditions. While the dielectric measurements are performed at constant temperature and variable frequency, the calorimetric investigations involve use of a linear temperature *vs.* time program to determine the heat capacity. With the help of temperature-modulated DSC [32] and heat capacity spectroscopy [33], it seems possible to perform isothermal measurements in an adequate frequency range to determine the complex heat capacity. It should then be possible to compare dielectric and calorimetric investigations directly to get information on possible differences between the responses due to electric and thermal perturbations. We intend to perform such measurements in the future.

References

1 D. Sappelt and J. Jäckle, J. Physics A-Mathematical & General, 26 (1993) 7325.
2 G. Adam and J. H. Gibbs, J. Chem. Phys., 43 (1965) 139.
3 P. Pissis, D. Daoukakidiamanti, L. Aspekis and C. Christodoulides, J. Physics-Condensed Matter, 6 (1994) L 325.
4 C. Schick and E. Donth, Physica Scripta, 43 (1991) 423.
5 E. Donth, Physica Scripta Volume T T49A, (1993) 223.
6 E. W. Fischer, E. Donth and W. Steffen, Phys. Rev. Letters, 68 (1992) 2344.
7 C. L. Jackson and G. B. McKenna, J. Non-Crystalline Solids, 131 (1991) 221.
8 J. Schüller, Y. B. Melnichenko, R. Richert and E. W. Fischer, Phys. Rev. Letters, 73 (1994) 2224.
9 R. Stannarius, F. Kremer and M. Arndt, Phys. Rev. Letters, (1995) accepted.
10 Y. Ishida, K. Yamafuji, H. Ito and M. Takayanagi, Kolloid-Zeitschrift & Zeitschrift für Polymere, 184 (1962) 97.
11 H. Suzuki, J. Grebowicz and B. Wunderlich, British Polym. J., 17 (1986) 1.
12 P. Cebe and P. P. Huo, Thermochim. Acta, 238 (1994) 229.
13 C. G. Vonk, J. Appl. Crystallog., 6 (1973) 81.
14 C. Schick, J. Wigger and W. Mischok, Acta Polymerica, 41 (1990) 137.
15 E. Donth, Glasübergang (Akademieverlag, Berlin, 1981).
16 T. A. Ezquerra, F. J. Baltacalleja and H. G. Zachmann, Polymer, 35 (1994) 2600.
17 G. Vigier, J. Tatibouet, A. Benatmane and R. Vassoille, Coll. Polym. Sci., 270 (1992) 1182.
18 S. Z. D. Cheng, M. Y. Cao and B. Wunderlich, Macromolecules., 19 (1986) 1868.
19 F. Fabry, Habilitationsschrift, PH Güstrow (1991).
20 C. Schick, F. Fabry, U. Schnell, G. Stoll, L. Deutschbein and W. Mischok, Acta Polym., 39 (1988) 705.
21 E. W. Fischer and S. Fakirov, J. Mater. Sci., 11 (1976) 1041.
22 G. Groeninckx, H. Reynaers, H. Berghmans and G. Smets, J. Polym. Sci. Polymer Physics Edition, 18 (1980) 1311.
23 G. Groeninckx and H. Reynaers, J. Polym. Sci. Polymer Physics Edition, 18 (1980) 1325.
24 C. Schick, L. Krämer and W. Mischock, Acta Polym., 36 (1985) 47.
25 S. Havriliak and S. Negami, J. Polym. Sci.; Part C, 14 (1966) 99.
26 E. Schlosser and A. Schönhals, Coll. Polym. Sci., 267 (1989) 963.
27 J. C. Coburn and R. H. Boyd, Macromolecul., 19 (1986) 2238.
28 A. Hensel, J. Dobbertin, J. Schawe, A. Boller and C. Schick, J. Thermal Anal., (accepted).
29 E. Donth, Relaxation and Thermodynamics in Polymers, Glass Transition Akademie Verlag, Berlin 1993.
30 A. Schönhals and E. Schlosser, Coll. Polym. Sci., 267 (1989) 125.
31 J. Jäckle, J. Non-Crystalline Solids, 172 (1994) 104.
32 J. Schawe, Thermochim. Acta, 261 (1995) 183.
33 N. O. Birge, S. R. Nagel, Rev. Sci. Instr., 58 (1987) 1446.